

## Scaling of Rheological Properties of Hydrogels from Associating Polymers

Lev Bromberg†

Center for Materials Science and Engineering, Massachusetts Institute of Technology, Cambridge, Massachusetts 02139

Received April 3, 1998; Revised Manuscript Received July 11, 1998

**ABSTRACT:** Rheological properties of thermoreversible hydrogels of poly(ethylene oxide)-*b*-poly(propylene oxide)-*b*-poly(ethylene oxide)-*g*-poly(acrylic acid) have been studied. The relaxation exponent  $\Delta = 0.69$  is found from the frequency-independent loss tangent at the gel point. The distance from the gelation threshold ( $\varepsilon$ ) is varied by changing the concentration or temperature. Dependencies of the zero-shear viscosity ( $\eta_0$ ) and equilibrium modulus ( $G_0$ ) scale as  $\eta_0 \sim \varepsilon^s$  and  $G_0 \sim \varepsilon^t$ . The transient exponents  $s = 1.26$ – $1.28$  and  $t = 2.64$ – $2.65$  are obtained in the vicinity of the gelation threshold. The scaling relation between *all* exponents is in excellent agreement with the Rouse model and is consistent with the percolation theory. Transient rheological properties exhibit complex scaling behavior above the gel point depending on  $\varepsilon$ . Scaling above the gel point correlates with the polymer structure.

### Introduction

Thermoreversible hydrogels attract lively research interest, despite their millennia-long history of use as food components.<sup>1–3</sup> The most seemingly obvious feature of thermoreversible hydrogels is their ability to gel, i.e., to transition, in a certain temperature region, from a viscous liquid to an assembly of infinite-molecular weight cross-linked molecules with significant elasticity. In many instances, like with proteins, the temperature-dependent gel formation is clearly observable at long time scales.<sup>4,5</sup> Many gels from synthetic associating polymers, however, possess very short relaxation times, which are difficult to observe.<sup>6</sup> These associating polymers usually comprise a water-soluble chain modified with a small number of hydrophobic moieties. Typically, a hydrocarbon or a fluorocarbon group used for modification is extremely hydrophobic.<sup>7,8</sup> The life-times of the associations between these hydrophobes, which are themselves water-insoluble at any temperature, decrease exponentially as the temperature increases.<sup>9</sup> On the other hand, since the entropy of the system drives hydrophobic interactions, the number of associations (and thus the viscosity) increases with temperature. Balance between the number of associations and their lifetime, i.e., dynamics, affects the strength of associations and ultimately thermogelation. Strongly associating hydrophobes may form micelle-like aggregates and the polymer will phase separate.<sup>10</sup> Conversely, weakly associating hydrophobes will not cause phase separation in a good solvent.

In the present work, the problem of scaling of rheological properties of hydrogels from associating polymers with complex temperature dependencies of viscosity is addressed. Recently, we have introduced a novel family of thermogelling materials where poly(acrylic acid) (PAA) segments are grafted onto Pluronic poly(ethylene oxide)-*b*-poly(propylene oxide)-*b*-poly(ethylene oxide) (PEO–PPO–PEO) block copolymers via C–C bonding.<sup>11–18</sup> Semidilute solutions of these materials show reversible gelation within a narrow temperature

range, with a gelled state having a significant storage modulus. Numerous, primarily medicinal, applications of these copolymers stem from their useful thermogelation ability.<sup>12,14</sup> Onset of gelation in Pluronic–PAA solutions coincides with augmentation of light scattering intensity of large scatterers and approaches the critical micellization temperature of the parent Pluronic.<sup>17</sup> PPO blocks serve as a hydrophobe in these materials. The transfer energy of the CH(CH<sub>3</sub>)CH<sub>2</sub>O– group from the aqueous to micellar phase is 4 times smaller at room temperature than the corresponding energy for a CH<sub>2</sub> group.<sup>19</sup> This “hydrophilicity” of PPO and its extremely temperature- and chain length-dependent interactions with water<sup>20</sup> require relatively long PPO blocks in order for the solution of a long (molecular weight 10<sup>5</sup>–10<sup>6</sup>) graft copolymer to gel. It is quite possible that when our polymers form solid-like networks, the PPO segments form multiple junctions.<sup>18</sup> The behavior of such polymer solutions is commonly described in terms of the theory of transient networks.<sup>21–26</sup> In a transient network, an association is stabilized by a binding energy, which must be overcome for the dissociation of the transient junction to occur. The average number of chains in the junction is determined by the balance between the chain disengagement and recombination rates. In the present study we were concerned with the relation between the experimentally found structure of our polymers and the scaling of rheological properties of their gels. Neither multiplicity of the junctions nor functionality of the PPO segment in our copolymers has been established, so that discussion in terms of the transient network theory<sup>25</sup> may not be well supported by observations.

As experiments pertaining to the present study were completed, a theory of thermoreversible gelation by Semenov and Rubinstein<sup>27,28</sup> was published. This theory considers solutions of polymer with many associating groups per chain. The dynamics of the network is governed primarily by the size of the water-soluble strand and by the effective lifetime of reversible junctions.<sup>28</sup> We believe that dynamics of dissociation and recombination of the PPO blocks can profoundly influence the viscosity and dynamic moduli of our gels.<sup>29</sup> We

† All correspondence should be directed to: 15 Sherwood Road, Swampscott, MA 01907. E-mail: cpbrolev@aol.com.

were thus tempted to relate obtained scaling exponents to the ones predicted by Semenov and Rubinstein.<sup>27,28</sup> As a result we were able to explain the dependence of transient scaling exponents on the distance from the gel point, both in the vicinity of the gelation threshold and beyond it.

## Experimental Section

**Materials.** Pluronic F127 NF was kindly donated by BASF Corp. (Parsippany, NJ) and used without further treatment. It has a formula EO<sub>100</sub>PO<sub>65</sub>EO<sub>100</sub>, nominal molecular weight 12 600, molecular weight of PPO segment 3780, 70 wt % of EO, and cloud point in 1% aqueous solutions above 100 °C. Acrylic acid (99%), lauroyl peroxide (97%), and dodecane (99+%) were purchased from Aldrich Chemical Co. (Milwaukee, WI) and used as received. Initiator 2,2'-azobis(2,4-dimethylpentanenitrile) was obtained from DuPont Specialty Chemicals (Wilmington, DE) and was recrystallized from cold acetone. Poly(vinylpyrrolidone-*co*-1-hexadecene) (Ganex V-216) (dispersion stabilizer) was obtained from International Specialty Products (Wayne, NJ) and used as received. All other chemicals, gases and organic solvents of the highest purity available were obtained from commercial sources.

**Synthesis.** Poly(ethylene oxide)-*b*-poly(propylene oxide)-*b*-poly(ethylene oxide)-*g*-poly(acrylic acid) was synthesized by dispersion/emulsion polymerization of acrylic acid along with simultaneous grafting of poly(acrylic acid) onto the Pluronic backbone, as described in detail elsewhere.<sup>16</sup> Briefly, an initiator system comprising a solution of lauroyl peroxide (140 mg) and 2,2'-azobis(2,4-dimethylpentanenitrile) (50 mg) in a small amount of acrylic acid was added into a solution of Pluronic (35 g) in partially neutralized acrylic acid (40 g). The resulting mixture was deoxygenated and introduced into a thermostated reactor charged with 400 mL of deoxygenated Ganex solution in dodecane. The emulsion was deoxygenated by nitrogen flow while stirring. Then reactor was heated to 70 °C and maintained at this temperature for 8 h under constant nitrogen flow while stirring. The resultant polymer was repeatedly washed with excess heptane and hexane in separation funnels and dried under vacuum at 40 °C. The polymer was fractionated at 15 °C by gel-permeation chromatography as previously described.<sup>16,17</sup> Molar masses of the fraction used in this work were  $3.15 \times 10^6$  ( $M_n$ ),  $3.61 \times 10^6$  ( $M_w$ ), and  $3.99 \times 10^6$  g/mol ( $M_z$ ). The polymer consisted of 43% Pluronic F127 and 57% poly(acrylic acid), as measured by FTIR and NMR.<sup>16,17</sup>

**Procedures.** To prepare solutions of Pluronic-PAA the polymer samples were dispersed in distilled water and gently stirred at 4 °C for 48 h. The pH was adjusted to  $7.4 \pm 0.1$  with 5 M NaOH as needed. The solutions were filtered through weighed Acrodisc nylon filters (Gelman Sciences, Ann Arbor, MI) with pore diameters of 0.8  $\mu$ m, deoxygenated by nitrogen flow, and stored at 4 °C. The polymer concentration in the solutions was controlled within  $\pm 0.005\%$ . Density of the degassed solutions (0–3%) was measured within a temperature range of 4–55 °C using a mercury-filled glass capillary dilatometer immersed into a programmable oil bath. Rheological measurements within the angular frequency ( $\omega$ ) range of 0.628 mrad s<sup>-1</sup> to 628 rad s<sup>-1</sup> (minimum strain  $6 \times 10^{-5}$ ) were performed using a controlled stress Rheolyst Series AR1000 rheometer (TA Instruments, New Castle, DE) with a cone and plate geometry system (cone: diameter, 4 cm; angle, 2°; truncation, 57  $\mu$ m) equipped with a solvent trap. Temperature control (internal resolution 0.016 °C) was provided by two Peltier plates. Equilibrium flow experiments were conducted in a stepped ramp mode with the shear stress as a controlled variable. Oscillatory shear experiments were performed in both frequency and temperature ramp modes. Minimum strain and stress were 0.0143% and 6 mPa, respectively. Zero-shear viscosity ( $\eta_0$ ) was computed by fitting  $\eta$  vs shear rate ( $\dot{\gamma}$ ) curves in the regions close to the low-shear plateau<sup>30</sup> using TA instruments and homemade software. The characteristic shear rate ( $\dot{\gamma}^*$ ) separating shear-independent and

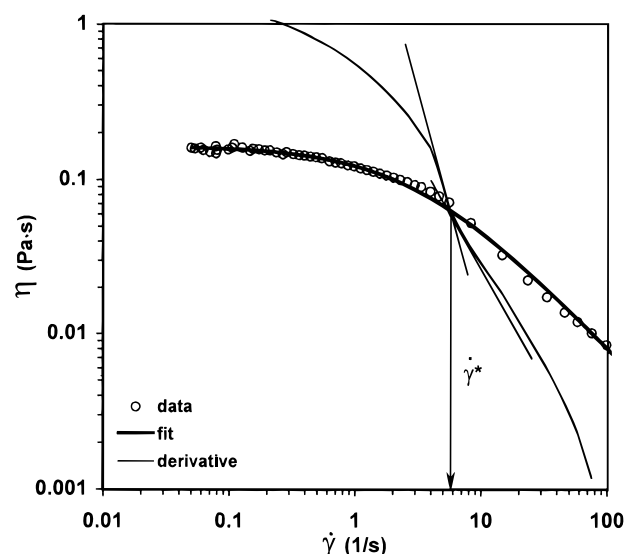


**Figure 1.** Equilibrium flow properties of 0.24% Pluronic-PAA aqueous solution at 37 °C and pH 7.4. Stepped torque ramp. The solid line is fitted to experimental data points using the Cross model at low strain rates:<sup>30</sup>

$$\eta = \frac{\eta_0 - \eta_\infty}{1 + (c\dot{\gamma})^i} + \eta_\infty$$

where  $\eta_0$  is the zero-rate viscosity,  $\eta_\infty$  is the infinite-rate viscosity,  $c$  is the consistency, and  $i$  is the rate index. Then derivative of the fit is calculated and is used to determine the characteristic shear rate ( $\dot{\gamma}^*$ ) as shown.

shear-thinning regions of viscosity was found from the first derivative of the algebraic fit of the  $\eta$  vs  $\dot{\gamma}$  plot (Figure 1). The  $\eta_0$  values were obtained for each solution in triplicate. Maximum standard deviations were 6%.

## Results and Discussion

**Scaling near the Gelation Threshold.** A clear rheological manifestation of the temperature-induced sol-gel transition in the solutions of Pluronic-PAA copolymers is an emergence of their elasticity above certain well-defined temperatures.<sup>17</sup> This transition is concentration-dependent (Figure 2). To quantify the critical gelation temperature ( $T_g$ ), a series of dynamic experiments was conducted at a fixed volume concentration ( $C = 1\%$ ) (Figure 3). As the temperature increases above  $T_g$ , the storage modulus ( $G'$ ) grows throughout the entire frequency range, reaching well-defined plateaus corresponding to the equilibrium moduli  $G_0$ .<sup>31</sup> Complex viscosity ( $\eta^*$ ) ascends accordingly; conversely, loss tangent  $\tan \delta = G''(\omega)/G'(\omega)$  decreases and becomes more frequency-dependent overall. This behavior, characteristic of the appearance of micelle-like clusters,<sup>17</sup> is limited by  $T_{gel}$  equivalent to  $T_e$  Nijenhuis' "maximum gelation temperature",<sup>3,32</sup> where these clusters dissociate on the observable time scale. The gel melting expressed itself in the decrease of  $G'$  and  $\eta^*$  above 45 °C (Figure 3). We thus limited our study of the gel scaling to  $T_g \leq T \leq 45$  °C. Appearance of well-defined  $G_0$  above 30 °C (Figure 3) indicates a temperature beyond the gelation threshold. Therefore, concentration-dependent scaling in gels was studied at 35 °C (Figure 4). Elastic moduli could be defined at  $C > 0.19\%$ ; below 0.19% the  $\tan \delta$  vs  $\omega$  plots showed a viscous liquid behavior. A series of minimum-strain, low-frequency experiments revealed phase boundaries between sol and gel states (Figures 5 and 6). Further discussion is concerned with data at  $T_g = 21.5$  °C,  $C_g =$

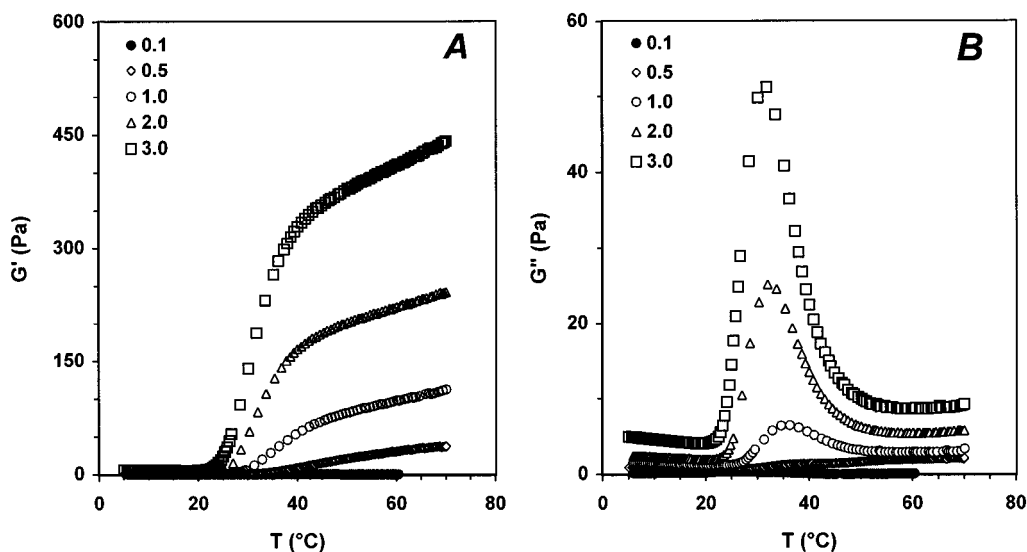


**Figure 2.** Temperature dependencies of storage modulus (A) and loss modulus (B) for Pluronic-PAA solutions during a heating ramp of 0.2 °C/min. Frequency of oscillatory shear 1 Hz, strain 0.01, pH 7.4. Numbers indicate concentration in v/v %.

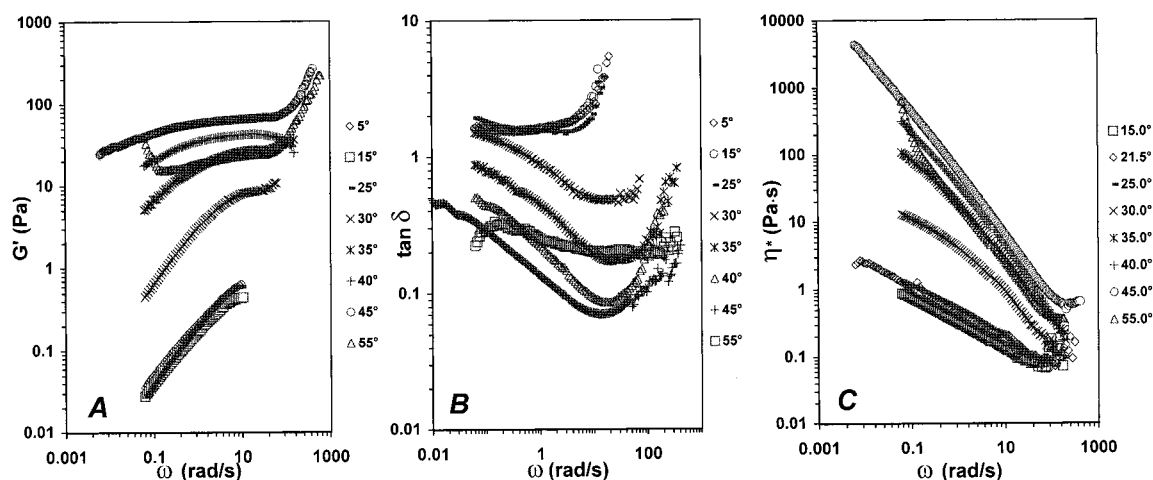


**Figure 3.** Storage modulus (A), loss tangent (B), and complex viscosity ( $\eta^*$ ) (C) of 1 v/v % Pluronic-PAA solutions as functions of angular frequency ( $\omega$ ) at different temperatures. A stress of 60 mPa is applied.

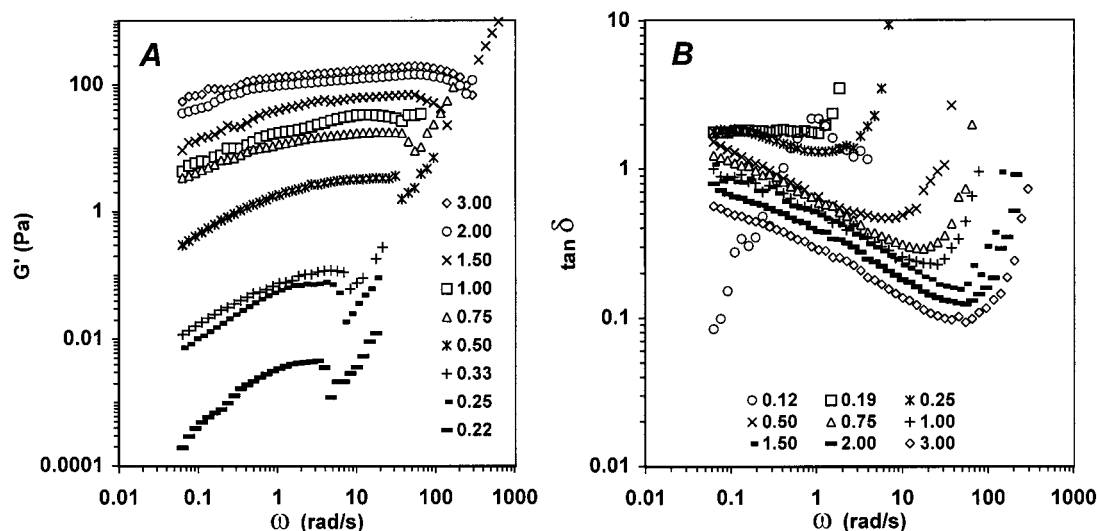


**Figure 4.** Concentration dependency of storage modulus (A) and loss tangent (B) for Pluronic-PAA gels during frequency ramp. Strain 0.001;  $T = 35$  °C. Numbers indicate concentration in v/v %.

0.19% (Figure 5). The relaxation exponent  $\Delta = 0.69$  was found from the frequency-independent  $\tan \delta = 1.87$  in

both temperature- and concentration-variation experiments by the Winter-Chambon method.<sup>33–37</sup>



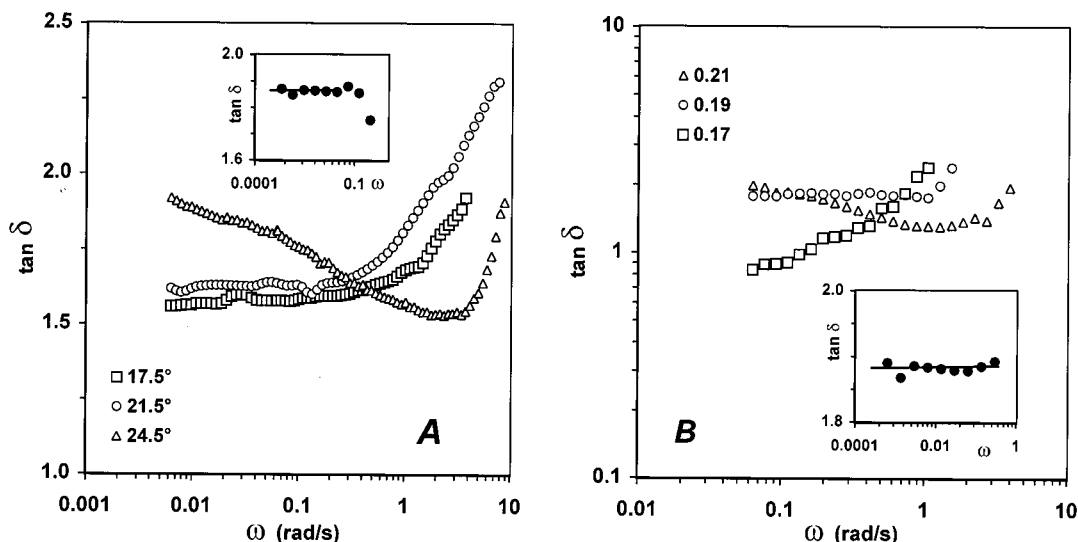


**Figure 5.** Temperature (A) and concentration (B) dependency of loss tangent for Pluronic-PAA solutions during frequency ramp. In (A), 1 v/v % solution is used. The inset shows the low-frequency region of the  $\tan \delta$  vs  $\omega$  plot at 21.5 °C. In (B), the temperature is 35 °C. Numbers indicate concentration in v/v %. The inset shows the low-frequency region of the  $\tan \delta$  vs  $\omega$  plot at  $C = 0.19\%$ . The oscillatory stress is 60 mPa (or 6 mPa in the inserts).

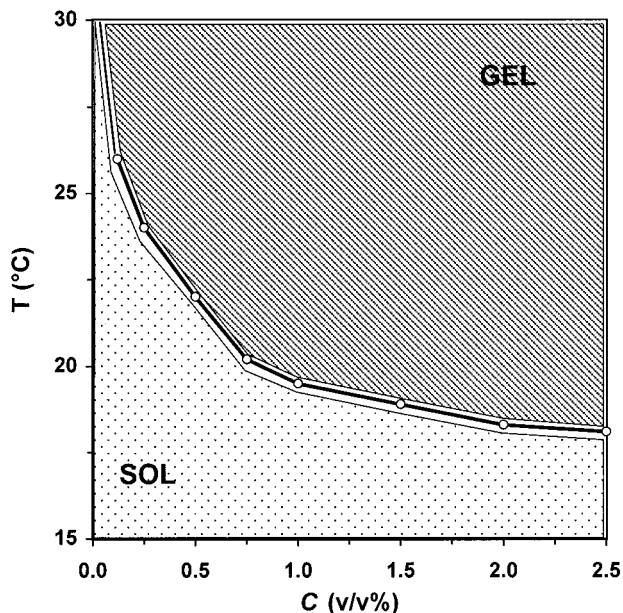


**Figure 6.** Phase diagram obtained at pH 7.4 for 1 v/v % copolymer solution by the Winter-Chambon method,<sup>35-37</sup> as illustrated in Figure 5.

$$\tan \delta_c = \frac{G''_c(\omega)}{G'_c(\omega)} = \tan \frac{\Delta\pi}{2} \quad \text{for} \quad 0 < \omega < 1/\tau_0, \quad p_{T_g, C_g} = p_c \quad (1)$$

where  $p$  is the degree of physical cross-linking,  $\tau_0$  is the characteristic relaxation time, and index  $c$  stands for the critical state at the gel point.

The value of the relaxation exponent  $\Delta$  found is close to the  $\Delta = 2/3$  predicted by Martin and Adolf<sup>38,39</sup> using percolation theory for the Rouse model where no hydrodynamic interactions are assumed. It is also in agreement with the  $\Delta = 0.71$ – $0.72$  predicted by de Gennes' electrical network analogy.<sup>40-45</sup> Various groups reported experimentally found  $\Delta = 0.66$ – $0.72$  for chemically cross-linked gels (for a review, see ref 31). Relatively fewer data have been reported on physical gels: Axelos and Kolb<sup>46</sup> found  $\Delta = 0.71$  for pectin in water,

Yu et al.<sup>47</sup> describe  $\Delta = 0.70$  for poly(methyl methacrylate)-polybutadiene triblock copolymers in *o*-xylene, and  $\Delta = 0.75$  was reported by Li et al.<sup>48-50</sup> for plasticized poly(vinyl chloride). It would appear that our finding adds further evidence to the validity of the scalar percolation theory prediction.

Can one relate the structure of the graft copolymers and experimentally found  $C_g$ ? On the basis of the Pluronic structure, the obtained ratio between Pluronic and acrylic acid, and the graft copolymer number-average mass (see Experimental Section), the gross formula of the Pluronic-*g*-PAA can be presented as  $[\text{EO}_{100}\text{PO}_{65}\text{EO}_{100}\text{AA}_{132}]_{142}$ .<sup>16</sup> The mechanism of synthesis where PAA chains grow off the Pluronic backbone<sup>17</sup> implies generation of ladder-like structures where the copolymer chain contains  $f$  hydrophobes (represented by PPO segments) separated by  $l$  water-soluble AA spacers. The length of a hydrophilic strand,  $l$ , is fundamentally analogous to the length of a subchain between cross-links in permanently cross-linked gels.<sup>51</sup> It has been our experience that within the temperature and concentration range under study no phase separations (followed by discontinuous volume changes) or polymer precipitation occurred, despite thermoreversible formation of micelle-like aggregates<sup>11-18</sup> (Figure 7). This observation can be easily explained by the extreme hydrophilicity of (neutralized) PAA, which constitutes strands between hydrophobes. This hydrophilicity expresses itself in swelling of the PAA strands, leading to very high excluded volume ( $\zeta$ ). Under good-solvent conditions,  $\zeta/a^3 \sim 1$ ,<sup>27</sup> where  $a$  is the effective monomer size ( $a^3 \cong 0.055 \text{ M}^{-1}$  for acrylic acid). The conversion  $p$  in the good-solvent system depends on the statistical weight of a bond between two associated hydrophobes ( $\lambda$ ):<sup>28</sup>

$$\frac{p}{(1-p)^2} \cong (\Gamma^1 C^{(1+\lambda)/(3\nu-1)}) \min(\lambda/a^3, f^{2+\lambda}) \quad (2)$$

The gelation concentration  $C_g^m$  at  $p(C_g^m) = p_g$  corresponds to the semidilute regime where the coils strongly overlap. It has been shown<sup>19,52</sup> that in our case  $C_g^m$  is much higher than  $c^*$  (the coil overlap concentration,

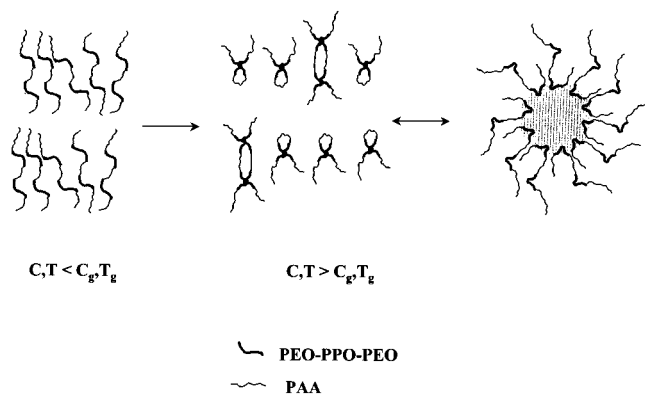


**Figure 7.** Scheme of associations between Pluronic-PAA chains. Above the gel point, intra- and interchain associations of Pluronic segments lead to formation of loops and micelles. We adopt an estimate of 10 for an average aggregation number of PPO segments in a core of the aggregate, as follows from the concurrent SANS study.<sup>13,15</sup>

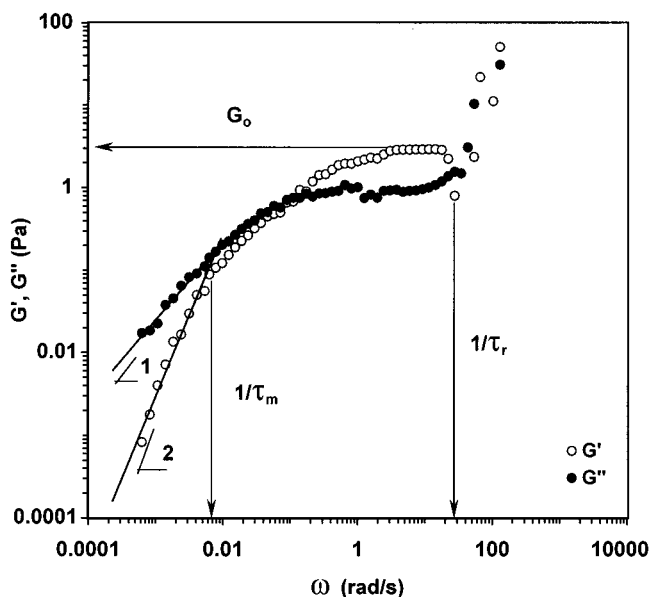


**Figure 8.** Dynamic moduli of a 0.5 v/v % Pluronic-PAA gel as functions of angular frequency at 37 °C. The oscillatory stress is 6 mPa. See text for other details.

which is equal to about 0.01 v/v%) and thus using eq 2 the monomer volume fraction can be estimated by<sup>27,28</sup>

$$C_g^m \sim l^{1-3\nu} f^{(1-3\nu)/(1+z)} \quad (3)$$

where  $\nu \cong 0.59$  is the Flory exponent for the good-solvent case<sup>42</sup> and  $z = \nu(3 + \theta_2) - 2 \cong 0.225$  (here  $\theta_2 \cong 0.78$  is the des Cloizeaux exponent<sup>53,54</sup>).

Using  $l = 132$ ,  $f = 142$  (see the gross formula above), eq 3 yields the estimate  $C_g^m \cong 0.001$ , in almost quantitative agreement with the experimentally obtained  $C_g^m = 0.0019 \times 0.57 = 0.0011$ . Here 0.57 is the fraction of acrylic acid in the polymer (see Experimental Section). This correlation prompted us to further seek a relationship between obtained scaling laws and the polymer structure.

**Scaling of the Dynamic Moduli above the Gelation Threshold.** In their study of pectin thermoreversible gels, Axelos and Kolb found that the dynamic moduli scale in the same way both below and above the gel point, as long as the distance from the gelation threshold ( $\varepsilon$ ) is not too large.<sup>46</sup> Indeed, at times shorter

than the relaxation time of a network strand ( $\tau_r$ ), but longer than the relaxation time of a free chain with no associated hydrophobes ( $\tau_{fc}$ ), the length scales are shorter than the strand lengths, and thus the dynamic moduli scale in the same way as below the gel point:<sup>28,31,46</sup>

$$G' \sim G'' \sim \omega \tau_{fc} \quad (4)$$

At time scales between  $\tau_r$  and  $\tau_m$  the system behaves as a cross-linked network, so that the storage modulus is almost constant at this regime:  $G' \cong G_0$ .<sup>28</sup> At times longer than  $\tau_m$  the system behaves as a liquid due to the network strand breakage.<sup>28,31</sup> Thus the scaling of the dynamic moduli can be described as<sup>28</sup>

$$G' \sim \begin{cases} \omega \tau_{fc}, & 1/\tau_r < \omega < 1/\tau_{fc} \\ \varepsilon^{(3\nu+z)/(3\nu-1)}, & 1/\tau_m < \omega < 1/\tau_r \\ (\omega \tau_m)^2, & \omega < 1/\tau_m \end{cases} \quad (5)$$

$$G' \sim \begin{cases} \omega \tau_{fc}, & 1/\tau_a < \omega < 1/\tau_{fc} \\ (\omega \tau_m)^{-1}, & 1/\tau_m < \omega < 1/\tau_a \\ (\omega \tau_m), & \omega < 1/\tau_m \end{cases} \quad (6)$$

where  $\tau_a = (\tau_m \tau_r)^{1/2}$  is the characteristic mean time scale.

A series of minimum-strain experiments within a wide range of frequencies was conducted to verify the character of  $\omega$ -dependencies of the dynamic moduli (Figure 8). Within the studied frequency range,  $G'$  and  $G''$  behaved as predicted by eqs 5 and 6. Below  $1/\tau_m$ ,  $G'$  and  $G''$  were proportional to  $\omega^2$  and  $\omega^1$ , respectively. Thus at low frequencies we observed behavior typical for Maxwell fluids and also characteristic of some hydrophobically modified polymers.<sup>55,56</sup> The zero-shear viscosity ( $\eta_0$ ) estimated from the relation  $\eta'_0 \sim G_0 \tau_m \cong 130$  Pa·s is within the same order of magnitude as  $\eta_0 \cong 50$  Pa·s found in equilibrium flow experiments at the same temperature and concentration. Hence, we believe the scaling behavior predicted by eqs 5 and 6 is valid for the system at hand. We thus proceeded to the study of scaling behavior of  $G_0$ .

It should be noted that the second term in eq 6 is valid at concentrations much higher than the gel point ( $C_g^m$ ) but lower than the concentration at which the hydrophilic spacers between chains strongly overlap ( $C_s$ ).<sup>28</sup> That is,  $\varepsilon_g \ll \varepsilon < \varepsilon_s$ . Above  $\varepsilon_s$ ,  $G_0 \sim \varepsilon$ . In the vicinity of the gelation threshold, but below the percolation concentration (i.e.,  $\varepsilon_g < \varepsilon < \varepsilon_{perc}$ ), the elastic modulus of the percolation network is

$$G' \sim G_0 \sim \varepsilon^{3\mu} \quad (7)$$

where  $\mu \cong 0.85$  is the percolation critical exponent.<sup>28</sup>

Both the second part of eqs 5 and 7 give similar value  $t = 2.55 - 2.59$  for the scaling of the equilibrium modulus. Experimental  $G_0$  vs  $\varepsilon$  plots (Figure 9) yielded  $t = 2.64$  and  $t = 2.65$  when the distance to the gel point was varied either by concentration ( $\varepsilon = C/C_g - 1$ ) or by temperature ( $\varepsilon_T = T/T_g - 1$ ), respectively. We believe this is in excellent agreement with the predicted values. The  $t$  values also agree very well with  $t = 8/3$  obtained by Martin and Adolf<sup>38</sup> for either Rouse or Zimm behavior based on scalar percolation theory. The  $t = 2.66 \pm 0.12$  and  $2.6 \pm 0.1$  have been also reported for pectin hydrogels<sup>46</sup> and plasticized poly(vinyl chloride),<sup>50</sup> respectively. It is unusual, however, that our gels

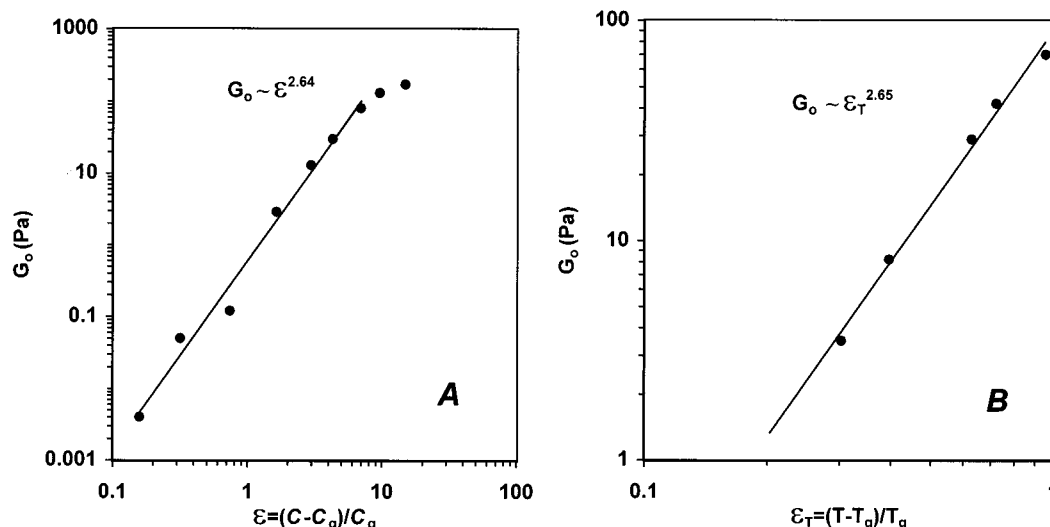


**Figure 9.** Scaling of equilibrium modulus ( $G_0$ ) obtained at different concentrations (A) and temperatures (B). In (A), the temperature is 35 °C. In (B), the concentration is 1 v/v %.

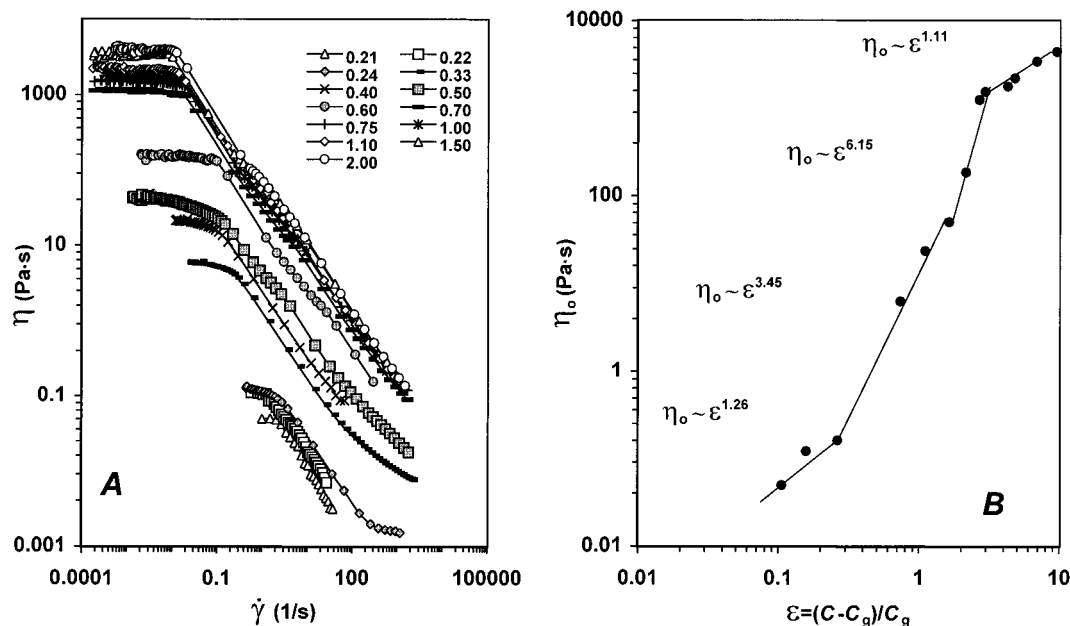


**Figure 10.** Scaling of gel viscosity at 37 °C as a function of concentration. In (A), experimental  $\eta$  vs  $\dot{\gamma}$  curves are presented. Numbers indicate concentration in v/v %. Each curve was fitted as shown in Figure 1. Calculated  $\eta_0$  values are plotted in (B) as a function of the distance to the gel point ( $\epsilon$ ). Straight lines represent scaling laws and are shown to guide the eye only. See text for other details.

appear to have similar scaling behavior, regardless of what parameter is varied, temperature or concentration (see also phase diagram in Figure 6). It is believed that this is the first reported encounter of such symmetry.

On the basis of the structure of our copolymers ( $I = 132$ ,  $f = 142$ ), we can predict at what distance from the gel point ( $\epsilon_s$ ) a weak  $G_0$  vs  $\epsilon$  dependence will be observed:

$$\epsilon_s \cong (I^{-3\nu})/C_g^m - 1 \cong 22 \quad (8)$$

A strong dependence of  $G_0$  vs  $\epsilon$  in Figure 9A starts to level off at  $\epsilon_s \cong 8$ , which is of the same order of magnitude as the predicted value (eq 8).

**Scaling of Viscosity above the Gelation Threshold.** Experimental data on  $\eta$  values above gelation threshold ( $C > 0.19\%$  at  $T = 37$  °C;  $T > 21.5$  °C at  $C = 1\%$ ) are presented in Figures 10 and 11. It is interesting

to observe that while in the shear-thinning region  $\eta$  vs  $\dot{\gamma}$  plots show similar slopes when either temperature or concentration is varied (Figures 10A and 11A), the  $\eta_0$  values differ by several orders of magnitude. It has been pointed out<sup>6</sup> that this lack of superposition is an occurrence common for strongly associating polymers.

To model the viscosity scaling above the gel point within as wide as possible a range of  $\epsilon$  and  $\epsilon_T$ , we will consider two regions of characteristic time scales.<sup>28</sup> The first region is associated with the lifetime of a strand of the reversible network ( $\tau_{\text{strand}}$ ), the elastic modulus of the reversible network ( $G_0$ ), and the zero-shear viscosity defined as  $\eta_0 \sim \tau_{\text{strand}} G_0$ . This region spans from above the gel point ( $\epsilon_g$ ) to critical concentrations ( $\epsilon_c$ ) somewhere below the percolation threshold ( $\epsilon_{\text{perc}}$ ). Here,  $\epsilon_{\text{perc}}$  indicates the limit of the range of validity of percolation statistics.<sup>28</sup> In the region  $\epsilon_{\text{perc}} > \epsilon$  the elastic modulus of the percolation network is  $G_0 \propto \epsilon^{3\nu}$ . The  $\epsilon_{\text{perc}}$

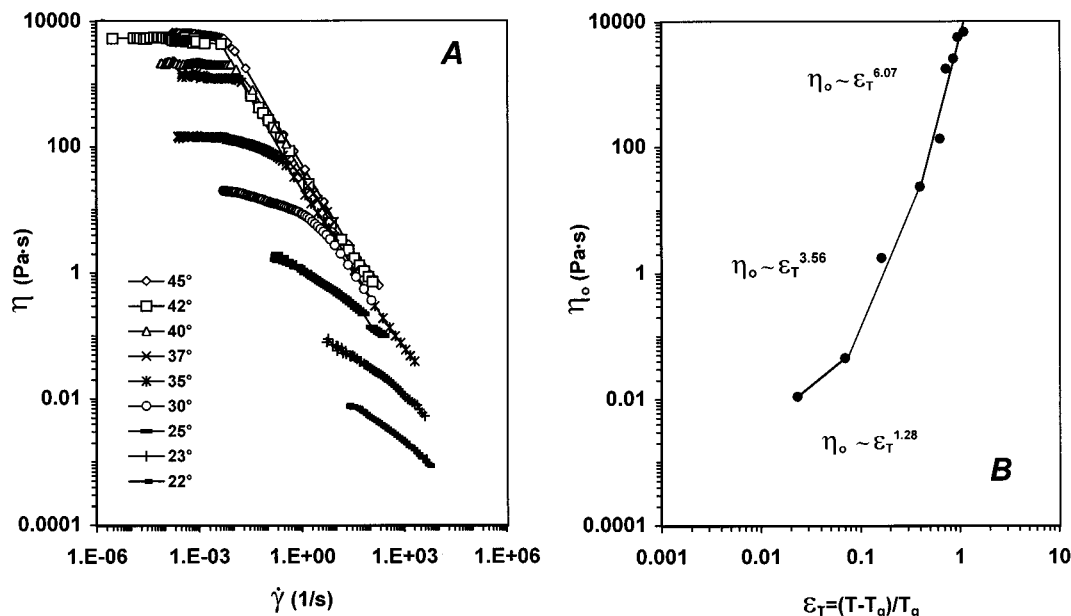


**Figure 11.** Scaling of 1/v % gel viscosity as a function of temperature. In (A), experimental  $\eta$  vs  $\dot{\gamma}$  curves are presented. Each curve was fitted as shown in Figure 1. The  $\eta_0$  values are plotted in (B) as a function of the distance to the gel point ( $\epsilon_T$ ). See Figure 10 and text for other details.

value is within the close distance to  $\epsilon_g$ .<sup>28</sup> Above  $\epsilon_{perc}$ , the Flory–Stockmayer mean-field theory holds.<sup>27,28</sup> The second region is associated with the chain relaxation time  $\tau_m$ , the modulus proportional to the concentration of chains ( $G_{chain}$ ), and the zero-shear viscosity dominated by the  $\tau_m$ :  $\eta_0 \sim G_{chain}\tau_m$ . This region starts at concentrations much higher than  $C_g$ . It has two scaling modes: one in the range when the concentration is below the overlap of the hydrophilic spacers between chains ( $\epsilon_g \ll \epsilon < \epsilon_s$ ), and another one above it ( $\epsilon > \epsilon_s$ ). In the vicinity of the gel point ( $\epsilon \rightarrow \epsilon_g$ ),  $\eta = \lim_{\omega \rightarrow 0} G''/\omega$ .

Following Rubinstein and Semenov,<sup>28</sup> we arrive at the following scaling scheme of the zero-shear viscosity:

$$\eta_0 \sim \begin{cases} \epsilon^{1/(3\nu-1)} \cong \epsilon^{1.30}, & \epsilon \rightarrow \epsilon_g \\ \epsilon^{1+(3\nu+z)/(3\nu-1)} \cong \epsilon^{3.59}, & \epsilon_g < \epsilon < \epsilon_c \\ \epsilon^{1+(3+3.5z)/(3\nu-1)} \cong \epsilon^{5.92}, & \epsilon_c < \epsilon < \epsilon_s \\ \epsilon^{1+0.5z/(3\nu-1)} \cong \epsilon^{1.15}, & \epsilon_s < \epsilon \end{cases} \quad (9)$$

The  $\epsilon_T$  values could be varied only within a relatively narrow range due to the gel melting above 45 °C (Figure 11), whereas the  $\epsilon$  values span about 2 orders of magnitude (Figure 10). It can be seen that both  $\eta_0$  vs  $\epsilon$  and  $\eta_0$  vs  $\epsilon_T$  plots could be approximated by exponent  $s = 1.26$ – $1.28$  in the vicinity of the gel point and  $s = 3.45$ – $3.56$  in the limited region above it. The  $\eta_0$  values scaled as  $\epsilon_T^{6.07}$  and  $\epsilon^{6.15}$  in the intervals  $\epsilon_T > 0.7$  ( $T > 30$  °C, Figure 11) and  $4 > \epsilon > 2$  ( $1\% > C > 0.5\%$ , Figure 10), respectively. At  $\epsilon \geq \epsilon_s > 4$ ,  $\eta_0 \sim \epsilon^{1.11}$  was observed. We can estimate  $\epsilon_{perc} \cong 0.7$ – $1.5$  and  $\epsilon_s \cong 4$ . The  $\epsilon_{perc}$  values are in agreement with the estimate

$$\epsilon_{perc} \cong f^{-(z/3)/(1+z)} \cong 0.74 \quad (10)$$

The  $\epsilon_s$  value corresponds, within 1 order of magnitude, with  $\epsilon_s \cong 22$  obtained from eq 8.

The structure of thermoreversible gels is in general much less dependent on their shear history than that of chemically cross-linked gels.<sup>27,46</sup> Therefore, we believe that the characteristic shear rate,  $\dot{\gamma}$ , corresponding

to the transition between shear-independent viscosity and the shear-thinning regime in our reversible hydrogels can reveal the dynamic critical exponent  $q$  relating  $\dot{\gamma}$  to the distance to the gel point:<sup>31,46</sup>

$$1/\dot{\gamma} \sim \epsilon^q \quad (11)$$

Scaling behavior of the characteristic shear rate vs  $\epsilon$  close to the gelation threshold is demonstrated in Figure 12. The dynamic critical exponent  $q = 3.80$ – $3.93$  was obtained.

We thus have determined all scaling exponents one can extract from a study of rheological properties. At this point the scaling relation between exponents within a relatively short distance from the gelation threshold can be verified:<sup>31</sup>

$$\begin{aligned} q &= s + t \\ \Delta &= \frac{t}{s+t} \end{aligned} \quad (12)$$

In eq 12, it is assumed that in our case the exponent  $s$  scales symmetrically both below and above the gel point.<sup>46</sup> With  $s = 1.27$ ,  $t = 2.65$ ,  $q = 3.87$ , and  $\Delta = 0.69$  the relation (12) holds quite accurately, hence corroborating the analysis of the scaling behavior by the Rouse model within the scalar percolation theory. We are aware of only one study of physical gels from pectin<sup>46</sup> where *all* scaling exponents were consistent with the percolation theory. No work is known in which scaling of rheological properties of thermoreversible *synthetic* hydrogels has been fully verified.

## Concluding Remarks

Rheological properties of semidilute solutions of poly(ethylene oxide)-*b*-poly(propylene oxide)-*b*-poly(ethylene oxide)-*g*-poly(acrylic acid) polymers of narrow polydispersity have been studied. These polymers are designed in accordance with the concept of the utilization of the poly(propylene oxide) segment as a temperature-sensitive group in hydrophobically-modified polymers.<sup>57</sup> Ex-



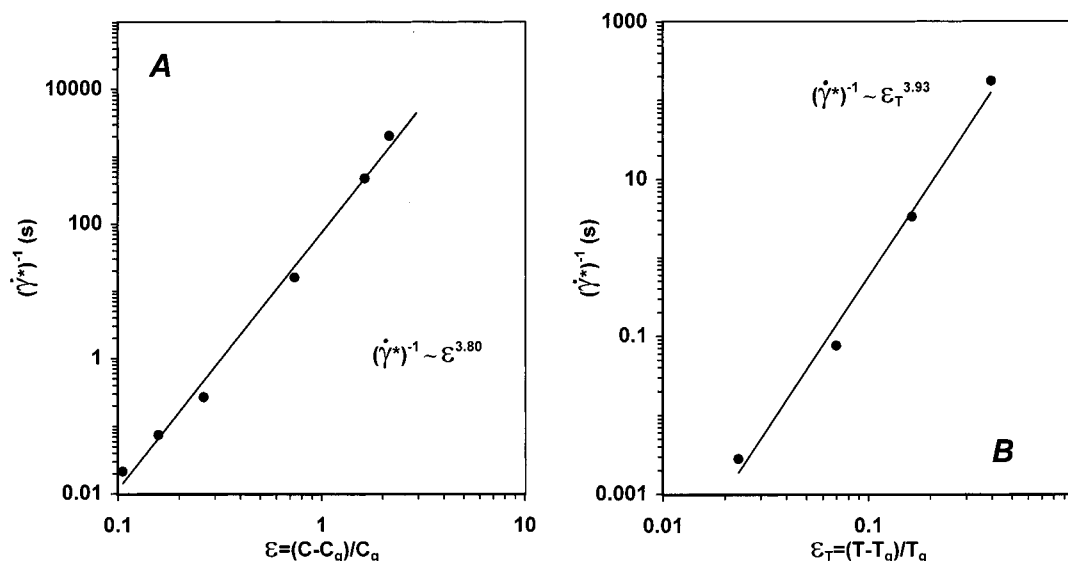


**Figure 12.** Scaling of characteristic shear rate ( $\dot{\gamma}^*$ ) obtained at different concentrations (A) and temperatures (B). In (A), the temperature is 37 °C. In (B), the concentration is 1 v/v %.

perimental evidence of the scaling behavior above the gel point passed through three main points: (i) The relaxation exponent  $\Delta = 0.69$  was found from the frequency-independent loss tangent in both temperature- and concentration-variation experiments by the Winter–Chambon method. (ii) Transient properties of hydrogels, such as zero-shear viscosity ( $\eta_0$ ) and equilibrium modulus ( $G_0$ ) revealed dependencies of the distance from the gel point ( $\varepsilon$ ), which scaled as  $\eta_0 \sim \varepsilon^s$  and  $G_0 \sim \varepsilon^t$ . The transient exponents  $s = 1.26$ – $1.28$  and  $t = 2.64$ – $2.65$  were obtained in the vicinity of the gelation threshold by varying either concentration or temperature. (iii) The scaling relation between exponents was in excellent agreement with the Rouse model within scalar percolation theory.

Transient rheological properties exhibited complex scaling behavior above the gel point depending on the power of  $\varepsilon$ . When concentration or temperatures are high enough, a strong power dependence of  $\varepsilon$  is observed:  $s \approx 3.45$ – $3.56$ . At concentrations and temperatures higher than the percolation distance ( $\varepsilon_{\text{perc}}$ ) but lower than the strand overlap distance ( $\varepsilon_s$ ), the exponent  $s \approx 6$  was obtained. At a still higher concentration when PAA strands overlap ( $\varepsilon_s$ ), the  $\eta_0$  vs  $\varepsilon$  dependence becomes weaker ( $s \approx 1.11$ ). These observations correspond very well to the Rouse regime where multiple hydrophobes on the same chain of the associative polymer may dissociate and recombine.<sup>27,28</sup> Based on the molecular weight and the hydrophobe content, the length of PAA chain between hydrophobes ( $l$ ) and the number of hydrophobes per chain ( $f$ ) were obtained. When used to predict the scaling behavior of  $\eta_0$  and  $G_0$ , the parameters  $l$  and  $f$  yielded the concentration at the gel point ( $C_g^m$ ), percolation distance ( $\varepsilon_{\text{perc}}$ ), and overlap distance ( $\varepsilon_s$ ), which matched well with the experimental values. It should be pointed out that since the grafting of the hydrophobe (Pluronic) onto growing PAA chains is random, the rheological properties of our copolymers depend on peculiarities of their synthesis, such as the hydrogen-abstracting power of the initiator, its concentration, etc.<sup>16,17</sup> Therefore, in the present work, special attention is paid to the use of the same fraction of the polymer that was characterized by the same PEO/PEO/PAA content and by the narrow polydispersity. The structure of the micelle-like aggregates and the effect

of the mean aggregation number on the gel rheology are described in our recent works.<sup>17,18,29</sup> The scaling laws found in the present study hold within a wide molecular weight range, as long as the polymer fractions differ only by the length of the PAA segments.<sup>18</sup>

**Acknowledgment.** The author is indebted to Prof. Michael Rubinstein for generous advice and to Dr. James Scott for careful editing of the manuscript.

## References and Notes

- (1) Clark, A. H.; Ross-Murphy, S. B. *Adv. Polym. Sci.* **1987**, *83*, 57.
- (2) Guenet, J.-M. *Thermoreversible Gelation of Polymers and Biopolymers*; Academic Press: London, 1992.
- (3) Te Nijenhuis, K. *Adv. Polym. Sci.* **1997**, *130*, 1.
- (4) Tobitani, A.; Ross-Murphy, S. B. *Macromolecules* **1997**, *30*, 4845.
- (5) Tobitani, A.; Ross-Murphy, S. B. *Macromolecules* **1997**, *30*, 4855.
- (6) Xu, B.; Yekta, A.; Winnik, M. A.; Sadeghy-Dalivand, K.; James, D. F.; Jenkins, R.; Bassett, D. *Langmuir* **1997**, *13*, 6903.
- (7) Targ, M.-R.; Kaszmariski, J. P.; Lundberg, D. J.; Glass, J. E. In *Hydrophilic Polymers. Performance with Environmental Acceptability*; Glass, J. E., Ed.; Advances in Chemistry 248; American Chemical Society: Washington, DC, 1996; Chapter 17.
- (8) Amis, E. J.; Hu, N.; Seery, T. A. P.; Hogen-Esch, T. E.; Yassini, Hwang, F. In *Hydrophilic Polymers. Performance with Environmental Acceptability*; Glass, J. E., Ed.; Advances in Chemistry 248; American Chemical Society: Washington, DC, 1996; Chapter 16.
- (9) Tanaka, F.; Edwards, S. F. *J. Non-Newtonian Fluid Mech.* **1992**, *43*, 247.
- (10) Semenov, A. N.; Joanny, J.-F.; Khokhlov, A. R. *Macromolecules* **1995**, *28*, 1066.
- (11) Bromberg, L.; Lupton, E. C.; Schiller, M. E.; Timm, M. J.; McKinney, G. W.; Orkisz, M.; Hand, B. Int. Pat. Appl. WO 97/00275, 1997.
- (12) Bromberg, L. E.; Ron, E. S. *Adv. Drug Delivery Rev.* **1998**, *31*, 197.
- (13) Huibers, P. D. T.; Lupton, E. C.; Bromberg, L. E.; Hatton, T. A. *Suppl. Chem. Eng. Prog., Annual Meeting of the American Institute of Chemical Engineers* **1997**, paper 93c.
- (14) Bromberg, L.; Orkisz, M.; Roos, E.; Ron, E. S.; Schiller, M. *J. Controlled Release* **1997**, *48*, 305.
- (15) Huibers, P. D. T.; Bromberg, L. E.; Lupton, E. C.; Hatton, T. A. Manuscript in preparation.
- (16) Bromberg, L. *Ind. Eng. Chem. Res.*, in press.
- (17) Bromberg, L. *J. Phys. Chem. B* **1998**, *102*, 1956.
- (18) Bromberg, L. *Langmuir*, in press.



- (19) Wanka, G.; Hoffmann, H.; Ulbricht, W. *Colloid Polym. Sci.* **1990**, **268**, 101.
- (20) Kjellander, R.; Florin, E. *J. Chem. Soc., Faraday Trans. 1* **1981**, **77**, 2053.
- (21) Green, M. S.; Tobolsky, A. V. *J. Chem. Phys.* **1946**, **14**, 80.
- (22) Clark, A. H.; Ross-Murphy, S. B. *Br. Polym. J.* **1985**, **17**, 164.
- (23) Tanaka, F.; Edwards, S. F. *Macromolecules* **1992**, **25**, 1516.
- (24) Tanaka, F.; Stockmayer, W. H. *Macromolecules* **1994**, **27**, 3943.
- (25) Tanaka, F.; Ishida, M. *Macromolecules* **1996**, **29**, 7571.
- (26) Tanaka, F. *Macromolecules* **1998**, **31**, 384.
- (27) Semenov, A. N.; Rubinstein, M. *Macromolecules* **1998**, **31**, 1373.
- (28) Rubinstein, M.; Semenov, A. N. *Macromolecules* **1998**, **31**, 1386.
- (29) Bromberg, L. *J. Phys. Chem. B*, in press.
- (30) Cross, M. M. *J. Colloid Sci.* **1965**, **20**, 417.
- (31) Adam, A.; Lairez, D. In *Physical Properties of Polymeric Gels*; Cohen Addad, J. P., Ed.; Wiley: New York, 1996; Chapter 4.
- (32) Te Nijenhuis, K. *Colloid Polym. Sci.* **1981**, **259**, 1017.
- (33) Chambon, F.; Winter, H. H. *Polym. Bull.* **1985**, **13**, 499.
- (34) Schwittay, C.; Mours, M.; Winter, H. H. *Faraday Discuss.* **1995**, **101**, 93.
- (35) Winter, H. H. *Prog. Colloid Polym. Sci.* **1987**, **71**, 104.
- (36) Mours, M.; Winter, H. H. *Macromolecules* **1996**, **29**, 7221.
- (37) Winter, H. H.; Mours, M. *Adv. Polym. Sci.* **1997**, **134**, 165.
- (38) Martin, J. E.; Adolf, D. *Annu. Rev. Phys. Chem.* **1991**, **42**, 311.
- (39) Martin, J. E.; Adolf, D.; Wilcoxon, J. P. *Phys. Rev. Lett.* **1988**, **61**, 2620.
- (40) de Gennes, P. G. *J. Phys. Lett.* **1976**, **37**, 1.
- (41) de Gennes, P. G. *J. Phys. Lett.* **1977**, **38**, 355.
- (42) de Gennes, P. G. *Scaling Concepts in Polymer Physics*; Cornell University Press: Ithaca, NY, 1979.
- (43) Efros, A. L.; Shklovskii, B. *Phys. Status Solidi B* **1976**, **76**, 47580.
- (44) Herrmann, H. J.; Derrida, B.; Vannimenus, J. *Phys. Rev.* **1984**, **B30**, 4080.
- (45) Laugier, J. M.; Luck, J. M. *J. Phys. A: Math. Gen.* **1987**, **20**, L885.
- (46) Axelos, M. A. V.; Kolb, M. *Phys. Rev. Lett.* **1990**, **64**, 1457.
- (47) Yu, J. M.; Dubois, Ph.; Teyssié, Ph.; Jérôme, R.; Blacher, S.; Brouers, F.; L'Homme, G. *Macromolecules* **1996**, **29**, 5384.
- (48) Li, L.; Aoki, Y. *Macromolecules* **1997**, **30**, 7835.
- (49) Li, L.; Uchida, H.; Aoki, Y.; Yao, M. L. *Macromolecules* **1997**, **30**, 7842.
- (50) Li, L.; Aoki, Y. *Macromolecules* **1998**, **31**, 740.
- (51) Bromberg, L.; Grosberg, A. Yu.; Matsuo, E. S.; Suzuki, Y.; Tanaka, T. *J. Chem. Phys.* **1997**, **106**, 2906.
- (52) Orkisz, M. J.; Bromberg, L.; Pike, R.; Lupton, E. C.; Ron, E. S. *Polym. Mater. Sci. Eng.* **1997**, **76**, 276.
- (53) des Cloizeaux, J.; Jannink, G. *Polymers in Solution*; Clarendon Press: Oxford, U.K., 1990.
- (54) des Cloizeaux, J. *J. Phys. Fr.* **1980**, **20**, 1935.
- (55) Annable, T.; Buscall, R.; Ettelaie, R.; Whittlestone, D. *J. Rheol.* **1993**, **37**, 695.
- (56) Annable, T.; Buscall, R.; Ettelaie, R. *Colloids Surf. A* **1996**, **112**, 97.
- (57) Bromberg, L. *Polymer* **1998**, **39**, 5663.

MA980523F